PHYSICAL REVIEW B VOLUME 50, NUMBER 11 15 SEPTEMBER 1994-I

Variations of the hole effective masses induced by tensile strain in $In_{1-x}Ga_xAs(P)$/InGaAsP heterostructures

R. W. Martin,* S. L. Wong, R. J. Warburton,† and R. J. Nicholas
Clarendon Laboratory, Parks Road, Oxford, OX1 3PU, United Kingdom

A. D. Smith, M. A. Gibbon, and E. J. Thrush
BNR Europe Ltd., London Road, Harlow, Essex, CM17 9NA, United Kingdom
(Received 28 April 1994)

Magneto-optical experiments have been used to study a range of InGaAsP-based multiple-quantum-well (MQW) structures containing biaxial strains, ranging from 1.6% tensile to 1.0% compressive. The observed excitonic transitions, involving both heavy and light holes, are studied in fields up to 15 T. Estimates of the hole effective masses are made, providing details of the valence-band nonparabolicities, and electronlike behavior is demonstrated for both heavy and light holes with different amounts of tensile strain. This is related to band crossings within the valence band and enables an estimate of 0.68 ± 0.10 to be made of the heterojunction band offset in a strained $In_{1-x}Ga_xAs$/InGaAsP MQW, with approximately 1.25% tensile strain in the well region. The experimental data are compared to the results of $\mathbf{k}\cdot\mathbf{p}$ Hamiltonian calculations of the in-plane valence-band dispersion.

INTRODUCTION

The incorporation of biaxial strains in multiple-quantum-well (MQW) structures allows greater freedom in the choice of the layer compositions and also leads to a number of possibilities for band-structure engineering. These have been demonstrated by improvements in the performance of quantum-well lasers, with either compressive or tensile strain, and of high-speed transistors. The strain breaks the degeneracy of the valence band at the Γ point, causing marked changes in the valence-band dispersion, hole effective masses, and heterojunction band lineups. Studies of strain modifications of the band structure and material parameters are required for the explanation and exploitation of such effects. This paper describes an investigation of strain effects in InGaAsP-based MQW using magneto-optical measurements. In particular, a systematic investigation of the effects of tensile strain on the effective hole masses and excitonic properties is reported.

For quantum wells under biaxial compressive strain the heavy-hole ($m_j=\frac{3}{2}$) band edge lies at a higher energy than that of the light holes ($m_j=\frac{1}{2}$), increasing the separation of the first heavy- (HH1) and light-hole (LH1) confined states relative to that in a lattice-matched structure. The uppermost HH1 level has a reduced in-plane effective mass, as has been measured in several systems [e.g., Refs. 1 and 2] leading to advantages for quantum-well lasers and high-speed transistors.[3] The decoupling of the hole subbands can dramatically simplify the properties of the valence band as seen, for example, in the demonstration of a two-dimensional (2D) quantization of spin for holes in compressively strained quantum wells.[4,5]

For small tensile strains the effect of the strain is to bring the HH1 and LH1 levels closer together and only for large strains is the energy of the LH1 level moved well above that of the HH1. Hence the coupling of the light and heavy holes is increased by small tensile strains, and a reduction of the in-plane effective mass is not expected. The observation[6] of improved laser performance using tensile strained quantum wells was therefore not anticipated and requires a very different explanation than that for the compressively strained material. O'Reilly *et al.*[7] have described such a mechanism, relating to the polarization properties of the confined holes. However, an alternative suggestion[8] is that the large well widths, required to achieve the desired wavelengths, result in LH1-HH1 splittings large enough to reduce the light-hole in-plane mass to a level similar to that of the heavy holes in a compressively strained laser. The laser performance would then be improved in a similar way as in compressively strained devices. Measured values for the hole effective masses as a function of tensile strain are scarce, but are important for clarifying such issues and for facilitating a greater understanding of the properties of strained layers in general.

With increasing tensile strain various level crossings can be induced in the MQW valence band, leading to complicated E-k dispersion curves and changes in effective mass. As mentioned above, small tensile strain counteracts the difference in quantum confinement for the heavy and light holes, and reduces the HH1-LH1 separation. At one particular magnitude of strain these levels become degenerate at the zone center ($k=0$). For larger tensile strains the LH1 level is the highest hole state, lying above the HH1 level, and further increase of the strain causes the HH1 and second light hole (LH2) levels to move together and eventually become degenerate. Strong mixing of the HH and LH states near such degeneracies can produce very large and/or electronlike hole effective masses, as demonstrated in this paper.

An experimental analysis of the strain dependence of

 ©1994 The American Physical Society

the in-plane effective masses and band structure in a series of tensile strained $In_{1-x}Ga_xAs(P)$/InGaAsP MQW structures, with comparative results from a compressively strained sample, is presented. Dramatic variations of the hole effective masses are demonstrated with negative values for both heavy and light holes at different strain values, along with changes in the excitonic absorption coefficients and binding energies. The observations reveal effects of the strain-induced band mixing, most notably near the HH1-LH2 crossover. To the best of our knowledge, this is the first experimental data relating to this degeneracy and enables the first estimate to be made for the band offset ratio in a tensile strained InGaAsP MQW structure.

Magnetoabsorption data is presented and calculations of the cyclotron splittings and diamagnetic shifts of the observed excitonic transitions are used to determine the reduced masses and binding energies of the excitons. Estimates of the effective hole masses can be made and are compared with $\mathbf{k}\cdot\mathbf{p}$ Hamiltonian calculations of the valence-band E-k dispersion near the zone center.

EXPERIMENTAL RESULTS

The InGaAsP-based MQW's were grown by low-pressure metalorganic vapor-phase epitaxy (MOVPE) at BNR Europe Ltd., on InP substrates. X-ray crystallography provided values for the quantum-well periods and the mean mismatch in the MQW region. A series of nine $In_{1-x}Ga_xAs$/InGaAsP structures was studied, each with a different tensile strain in the well region. The samples contain four quantum wells, nominally 95-Å wide, between 140-Å-thick $In_{0.82}Ga_{0.18}As_{0.39}P_{0.61}$ barriers, lattice matched to the InP. The measured quantum-well strains range from $+0.15\%$ to $+1.56\%$ corresponding to gallium contents of between 49% and 70% in the $In_{1-x}Ga_xAs$. A strain-compensated $In_{0.81}Ga_{0.19}As_{0.73}P_{0.27}/In_{0.61}Ga_{0.39}As_{0.53}P_{0.47}$ six-period MQW, in which the wells and barriers are nominally of equal width and are under 1% compressive and 1% tensile strain, respectively, was also studied. The x-ray data for this sample indicated a MQW period of 184 Å and a mean MQW strain of -0.16%. In addition, a number of lattice-matched $In_{1-x}Ga_xAs$/InGaAsP and InGaAsP/InGaAsP MQW's were also measured. This range of quantum-well biaxial strain resulted in observed HH1-LH1 splittings from $+63$ to -99 meV. This region includes the degeneracies of the HH1 level with both the LH1 and LH2 levels.

Absorption spectra were measured at 4.2 K for each of these structures, in magnetic fields of up to 15 T. In each case the $E1$-HH1 and $E1$-LH1 excitonic transitions, along with a number of associated Landau levels, were resolved. Transitions involving higher confined levels were observed in some samples. The absorption coefficient per well, measured at zero field, for a number of the samples is illustrated in Fig. 1. The lattice-matched $In_{0.57}Ga_{0.43}As_{0.92}P_{0.08}/In_{0.81}Ga_{0.19}As_{0.41}P_{0.59}$ sample, as shown in Fig. 1(b), illustrates the familiar case where the $E1$-HH1 exciton appears stronger, and lower in energy, than that of the $E1$-LH1. The $E1$-HH1 transition has been shifted to a much lower energy than that of the $E1$-LH1 in the InGaAsP/InGaAsP structure with compressively strained wells; see Fig. 1(a). A broad $E2$-HH2 transition can also be seen in both of these samples. For the $In_{1-x}Ga_xAs$/InGaAsP sample with the least tensile strain ($\varepsilon_{well}=0.15\%$) the $E1$-HH1 transition still appears at a lower energy than that of the $E1$-LH1, but for wells with relatively large tensile strains ($\varepsilon_{well}>0.3\%$) this order is reversed due to the effect of the strain on the band-edge positions as discussed above. Of particular interest is the structure with $\varepsilon_{well}=0.28\%$, shown in Fig. 1(c), for which the $E1$-HH1 and $E1$-LH1 are approximately coincident, with the strain-induced HH1-LH1 splitting canceled by that resulting from quantum confinement. Figures 1(d) and 1(e) show data from MQWs with larger tensile strains ($\varepsilon_{well}=1.0\%$ and 1.2%) for which the $E1$-HH1 transition has shifted to a much higher energy than that of the $E1$-LH1.

The splitting of the HH1 and LH1 levels is plotted in Fig. 2 as a function of ε_{well} for all of the samples measured. The solid line shows reasonable agreement with the results of an envelope function calculation of the confined energy levels, using material parameters interpolated from values for the four constituent binaries. Such a calculation requires values for the heterojunction band offsets as a function of strain and composition. These have been estimated using the "model solid" theory,[9] which employs deformation potentials to account for the effects of strain. The model requires values for the "aver-

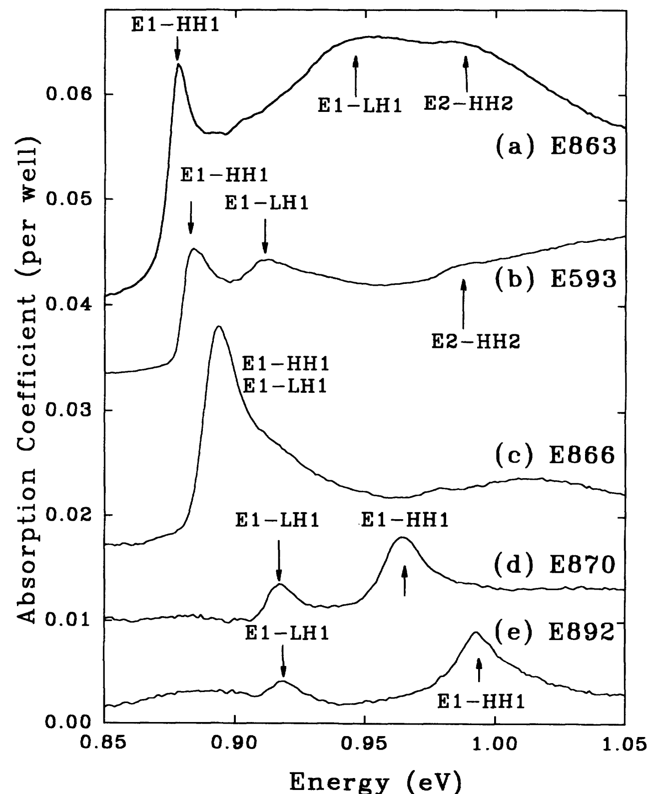

FIG. 1. The absorption coefficient per well measured at 4.2 K for a range of InGaAS(P)/InGaAsP MQW samples incorporating a range of different strains.

age" valence-band positions and these are obtained by interpolation of the tabulated binary parameter using bowing parameters calculated as in Ref. 10. However, it should be noted that the quality of the fit in Fig. 2 is quite insensitive to the values used for the band offset ratios, as a result of tradeoffs between the electron and hole confinement energies, and accurate estimates of the band offset ratios are not possible. An estimation of the band offset ratio in one of the tensile strained structures, based on the observation of level crossings in the valence band, will be discussed below and is found to be considerably different to the estimate made by the method described above.

When a magnetic field is applied perpendicular to the sample the $E1$-HH1 and $E1$-LH1 excitons each generate a series of Landau-level transitions, as seen in the transmission spectra for $\varepsilon_{\mathrm{well}}=-1.0\%$ and $+0.97\%$ (Fig. 3). For the structure with tensile strain ($\varepsilon_{\mathrm{well}}=-0.97\%$) the $E1$-LH1 transition occurs at 916 meV, approximately 48 meV below the $E1$-HH1 minimum, with the strong feature near 1130 meV arising from the bulklike InGaAsP layers on either side of the MQW stack. The $E1$-HH1 1*s* transition is seen to be considerably stronger than that of the $E1$-LH1, as expected from the 3:1 ratio in HH/LH excitonic absorption strengths resulting from the form of the Bloch functions. However, it is the light-hole Landau levels which dominate, even at energies 150 meV above the $E1$-HH1 transition. These strong light-hole levels are characteristic of the more highly strained tensile strained samples, in marked contrast to the complete dominance of the heavy-hole Landau levels observed for the compressively strained wells, as seen in Fig. 3 for $\varepsilon_{\mathrm{well}}=-1.0\%$. For this sample the $E1$-HH1 transition appears well below that of the $E1$-LH1 and a single series of heavy-hole Landau levels can be resolved over an energy range of 200 meV at 15 T. The observed transitions are plotted as a function of magnetic field in Fig. 4 for the $\varepsilon_{\mathrm{well}}=-1.0\%$, $+0.26\%$, and $+0.97\%$ strained MQW samples. For the compressively strained wells, in Fig. 4(a), the single series of heavy-hole Landau levels are indicated, while in Figs. 4(b) and 4(c) separate series of Landau levels for the heavy- and light-hole excitons can be identified at low energies.

The magnitude of the cyclotron splittings between the ground and first excited states at 12 T are shown in Fig. 5 for all the samples measured. This largely represents the sum of the electron and hole cyclotron energies, with only a small contribution from the excitonic binding energy. Figure 5 demonstrates a strong dependence of this cyclotron splitting for the heavy-hole excitons on the strain in the quantum-well region, corresponding to

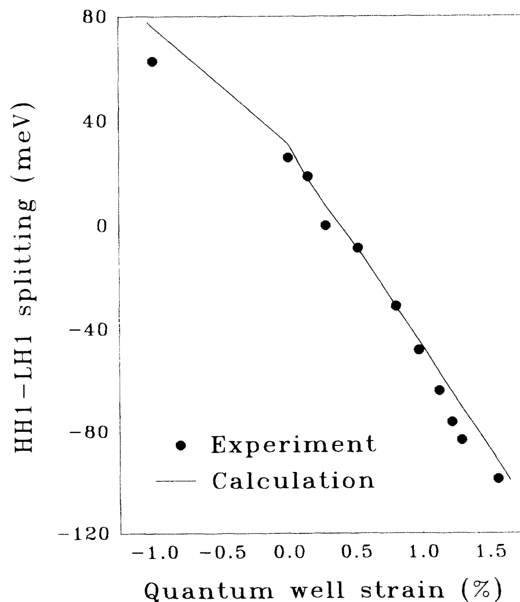

FIG. 2. The splitting of the HH1 and LH1 energy levels as measured at 4.2 K. The first two data points correspond to InGaAsP/InGaAsP MQW structures and the remainder to the series of tensile strained InGaAs/InGaAsP samples. The solid line shows the results from a calculation as described in the text.

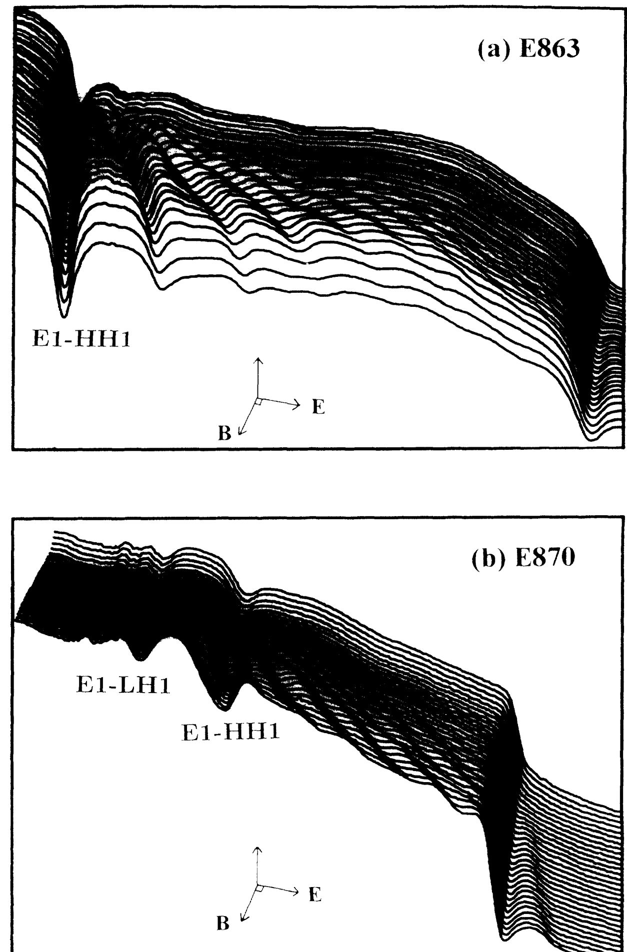

FIG. 3. Magnetotransmission spectra from (a) a strain balanced InGaAsP/InGaAsP MQW with 1% compressive strain within the well region and (b) a tensile strained InGaAs/InGaAsP MQW with $\varepsilon_{\mathrm{well}}=+0.97\%$. The magnetic field decreases in 0.5 T steps from 15 T (front trace) to 0 T (back trace) and the traces have been rotated for clarity.

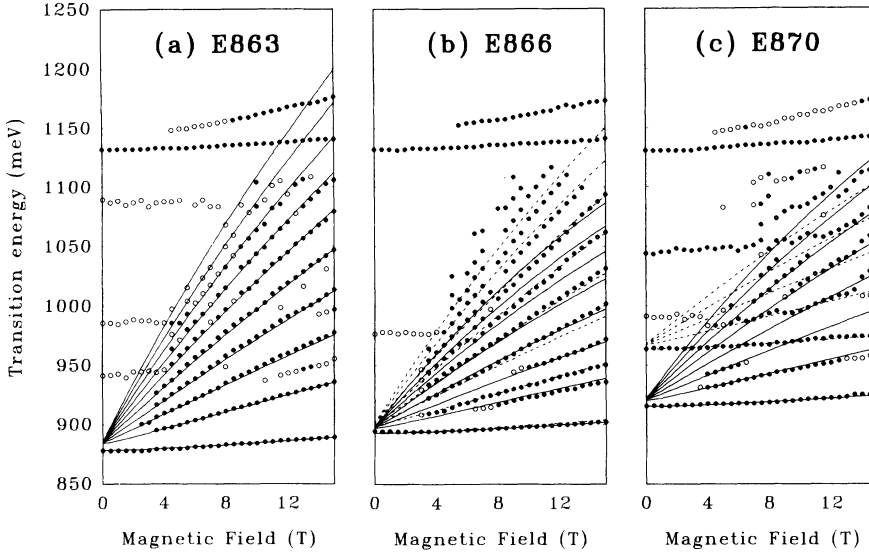

FIG. 4. Fan diagrams showing the excitonic transition observed in magnetic fields up to 15 T for three of the samples (E863, E866, and E870, respectively). The solid circles correspond to well-resolved features, while the open circles indicate weak or broad transitions. The lines are the results of the fitting procedure described in the text.

changes in the excitonic reduced mass. The excitonic Landau-level energies are fitted using the results of a variational calculation of a 3D hydrogeniclike exciton in a magnetic field.[11] The in-plane hole effective masses and exciton binding energies can be estimated, having accounted for the effects of conduction-band nonparabolicity and of variations in electron effective mass as a function of strain and composition. After using an interpolation formula to compute values of the bulk band-edge electron mass $[m^{\mathrm{unstr}}(0)]$ as a function of layer composition, the following $\mathbf{k}\cdot\mathbf{p}$ expression for the strained in-plane electron mass $[m^{\mathrm{str}}(E)]$ is used to account for the above band-edge energy resulting from electric and magnetic quantization:

$$\frac{m^{\mathrm{str}}(E)}{m^{\mathrm{unstr}}(0)}=\frac{(E+E_0^{\mathrm{str}})(E+E_{\mathrm{so}}^{\mathrm{str}})(E_0^{\mathrm{unstr}}+\frac{2}{3}\Delta)}{(E+\frac{1}{3}E_0^{\mathrm{str}}+\frac{2}{3}E_{\mathrm{so}}^{\mathrm{str}})(E_0^{\mathrm{unstr}})(E_0^{\mathrm{unstr}}+\Delta)}\;,$$

$$E=E1+[(n+\tfrac{1}{2})\hbar\omega_B]\;,$$

where E_0 is the fundamental band gap, E_{so} is the energy gap between the conduction band and the spin-orbit band, Δ is the unstrained bulk spin-orbit splitting, $E1$ is the confinement energy for the first electron level, n is the Landau-level index, ω_B is the cyclotron energy, and the superscripts str and unstr correspond to strained and unstrained material, respectively.

This enables the observed heavy-hole and light-hole Landau levels to be fitted using an excitonic binding energy and in-plane hole effective mass as the adjustable parameters in each case. The result of such a procedure is illustrated by the fitted lines in Fig. 4 and the best estimates for the in-plane hole effective masses and exciton binding energies for all the samples are summarized in Table I. The estimated uncertainties resulting from this process are typically $\pm 0.25(m_0^{-1})$ for the inverse hole effective masses and ± 2 meV for the binding energies.

The estimated binding energies do not change greatly with strain, with those for the light-hole exciton generally

TABLE I. Values of the hole in-plane effective masses, excitonic binding energies, and excitonic reduced masses estimated using the magnetoabsorption data from a series of strained InGaAs(P) MQW's.

Sample number	Gallium content (%)	Biaxial strain (%)	In-plane hole effective mass HH (m_0)	In-plane hole effective mass LH (m_0)	Excitonic binding energy HH (meV)	Excitonic binding energy LH (meV)	Excitonic reduced mass HH (m_0)	Excitonic reduced mass LH (m_0)
E863	19[a]	−1.00	0.185		8		0.0414	
E593/E839	43[a]	0	0.45		8		0.0449	
E874	49	+0.15	0.70	−0.20	7	7	0.0423	0.0582
E866	51	+0.28	0.40	−0.45	9	6	0.0406	0.0502
E868	54	+0.52	0.50	−0.50	6	7	0.0416	0.0499
E869	58	+0.80	0.90	−1.00	5	6	0.0432	0.0476
E870	61	+0.97	−1.00	−0.80	5	7	0.0477	0.0482
E876	63	+1.12	−0.30	−0.40	5	6	0.0537	0.0514
E892	65	+1.21	−0.23	−0.50	6	6	0.0570	0.0503
E878	66	+1.29	0.35	−0.40	5	7	0.0404	0.0516
E898	70	+1.56		−0.45		5		0.0510

[a]InGaAsP quaternary.

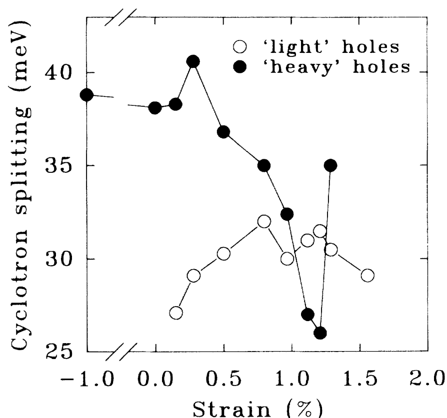

FIG. 5. The cyclotron splitting of the ground and first excited state measured at 12 T as a function of strain within the quantum-well region.

higher than for the heavy-hole exciton. However, marked changes in the sign and magnitude of the effective masses are seen. A clearer picture emerges from a plot of the inverse effective masses for the heavy and light holes as a function of $\varepsilon_{\rm well}$, as shown in Fig. 6. This is similar in form to the plot of measured cyclotron splittings in Fig. 5, and although uncertainties in the electron masses and nonparabolicities could shift the zero line ($m^* = \infty$), these will not change the overall shape of the curve. For compressive strain ($m^*=0.185m_0$) the in-plane heavy-hole mass is comparatively light compared to the bulk unstrained value ($m^*=0.43m_0$), as expected. For moderate tensile strains ($0.25\% < \varepsilon_{\rm well} < 0.50\%$) the heavy-hole masses are close to the bulk values, but for greater strains the mass increases rapidly and above $\varepsilon_{\rm well} \approx 1\%$ swaps over to become negative. In the region

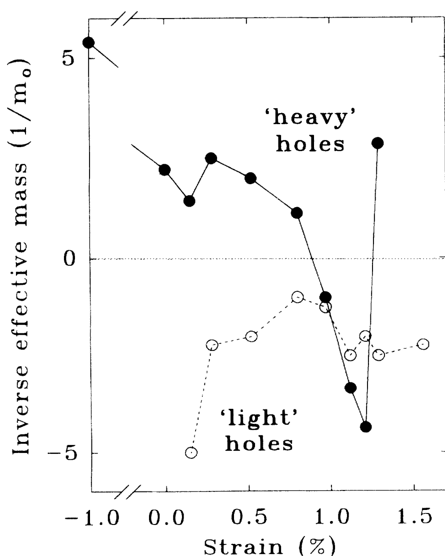

FIG. 6. The inverse effective masses estimated, as described in the text, for the light and heavy holes as a function of strain within the quantum-well region.

of 1.25% there is a discontinuity where the mass suddenly becomes light and positive, which we associate with the crossing of the HH1 and LH2 levels as described below. By contrast there is relatively little change in the light-hole effective masses, which remain electronlike for all the tensile strained samples with a value close to $-0.45m_0$ for $\varepsilon_{\rm well} > 1.0\%$. The well widths of 95 Å are below those used for tensile strained 1.55-μm lasers, but there is no evidence of a reduction in the light-hole masses. Although similar experimental data is rare, a recent report of magneto-optical studies of tensile strained $Ga_{1-x}As_xP/Al_{1-x}Ga_xAs$ structures, over a much smaller range of HH1-LH1 splittings, demonstrates large valence-band masses when this splitting approaches zero.[12]

The magnitude of the excitonic reduced mass, μ, has an important effect on the optical absorption, through changes in the overlap probability of the electron and hole in the exciton.[13] Large or negative values of the light-hole in-plane effective masses in tensile strained quantum wells will increased μ, giving a reduced excitonic radius and leading to enhanced excitonic oscillator strength. The excitonic absorption coefficient is proportional to μ^2 and thus, although μ is dominated by the lighter electron mass, an increase in hole mass will still produce a significant change in the absorption. The electronlike behavior of the holes leads to the possibility of extreme effects since a negative hole effective mass, similar in magnitude to that of the electrons, corresponds to extremely large values of μ resulting from electron and hole E-k dispersion curves that are approximately parallel over the appropriate region of k space, and greatly enhanced absorption is predicted. Clearly the simple two-particle exciton model will not apply for such a condition but large increases in absorption would still result. The maximum absorption coefficient per well for the $\varepsilon_{\rm well} = +0.28\%$ structure, with an estimated light-hole effective mass of $-0.45m_0$, is seen to be approximately double that of the lattice-matched sample [Figs. 1(b) and 1(c)]. The integrated intensity is also increased, but more work is required to examine the extent of this increase and to separate the contributions of the light- and heavy-hole excitons. A similar increase in absorption coefficient is seen for the compressively strained InGaAsP wells of Fig. 1(a), for which the estimated mass is only $0.185m_0$. This is due to an increased overlap of the electron and hole envelope functions, giving enhanced absorption coefficients for strain of either sense. These characteristics of strained material are potentially important for devices, such as modulators, whose operation depends on the strength of the optical absorption.

BAND-STRUCTURE CALCULATIONS

The values estimated above for the hole masses are average effective masses for a small region of k space near the zone center, and the changes reflect strain-induced changes in the valence-band dispersion near the Γ point. They are therefore compared with calculations of the in-plane E-k dispersion, performed using the Luttinger-Kohn Hamiltonian, as shown in Fig. 7 for a range of 90-

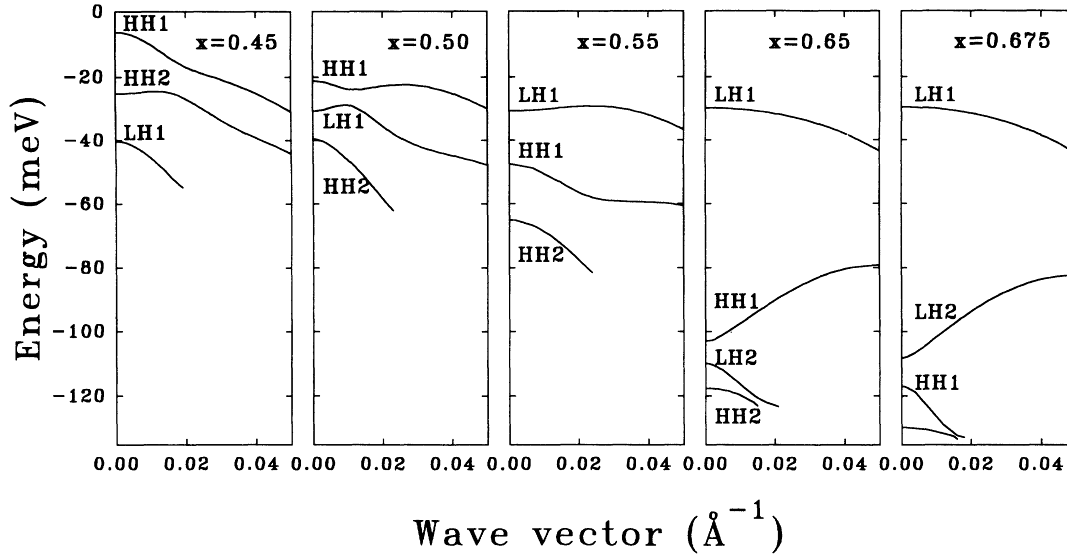

FIG. 7. In-plane valence-band dispersion calculated using the Luttinger-Kohn Hamiltonian for a range of tensile strained $In_{1-x}Ga_xAs$/InGaAsP MQW structures. The gallium contents within the wells are shown on the diagram and the zero of the energy scale is at the band edge of the highest valence band (LH in all but the first case).

Å $In_{1-x}Ga_xAs$ wells sandwiched between lattice-matched InGaAsP barriers. Structures with $x=0.45$, 0.50, 0.55, 0.65, and 0.675 are shown, covering a range of quantum-well strains from slightly compressive to strongly tensile (1.4%) and including the situations where the first heavy-hole level (HH1) interacts strongly with the LH1 and LH2 levels. As discussed elsewhere in this paper the strained heterojunction band offsets are not well known and for this calculation have been estimated by linear interpolation between the values for the lattice-matched case and that for which the HH1 and LH2 levels are degenerate (see below).

On changing from the slightly compressively strained case ($x=0.45$) to the first tensile strained sample ($x=0.50$) the LH1 level is seen to pass the HH2 level and approach the HH1 level. The band couplings result in a large heavy-hole mass and an electronlike light-hole mass, as observed for samples E874 and E866 ($x=0.49$ and 0.51). The LH1 level is the highest valence-band state for the $x=0.55$ structure, lying nearly 20 meV above the HH1 level. Coupling between these two levels, at finite values of k, results in a very flat and electronlike dispersion for the light holes, giving a large, negative effective mass. Table I shows that this is in agreement with the data from the $x=0.54$ and 0.58 samples, for which estimates of $-0.5m_0$ and $-1.0m_0$ were made. The corresponding values for the heavy-hole masses are $0.5m_0$ and $0.9m_0$, respectively. The data in Table I indicates that a further increase in tensile strain leads to an electronlike heavy-hole mass and the $x=0.65$ structure in Fig. 7 shows that this is due to coupling with the second light-hole level. The LH2 level has odd parity and couples strongly to the even-parity HH1 level, due to the k_z-dependent off-diagonal term in the Hamiltonian. The strain dependence of the effective mass is not expected to be so strong near the LH1-HH1 band crossing, since these levels are of the same parity and thus couple more weakly. The small, negative effective HH mass ($-0.23m_0$) estimated for E892 is in very good agreement with the calculated valence-band dispersion. The LH1 level is now approximately 70 meV above that of the HH1 but still retains a relatively heavy effective mass, clearly much larger than that of the HH1 band in the nearly lattice-matched structure ($x=0.45$). The very small light-hole cyclotron energy that will result is observed in the experimental data E892, although an electronlike mass was predicted. The calculated dispersion for the $x=0.675$ structure shows how a small increase in tensile strain causes the HH1 level to move below the LH2 level and dramatically changes the heavy-hole effective mass to light and positive, as observed in the experimental data from E878. It is anticipated that the difference between the measured light-hole effective masses and the E-k curves calculated for the two most highly strained structures could be resolved by including in the valence-band Hamiltonian a C_4 term, proportional to the axial strain and in-plane wave vector and significant only for tensile strained structures.[14]

The separation of the LH2 and HH1 levels is very dependent on ε_{well} and the electronlike mass for the heavy holes would be expected for only a narrow range of strains, as observed in Fig. 6. As the energy of the LH2 energy approaches that of the HH1, with increasing ε_{well}, the greater LH2-HH1 band mixing increases the curvature of the heavy-hole E-k dispersion, reducing the magnitude of the negative effective mass. For larger strain ($\varepsilon_{well} > 1.25\%$ in Fig. 6) the HH1 level crosses to a lower energy than LH2 and its E-k dispersion curve is once again holelike, giving a light but positive effective heavy-hole mass. The LH2-HH1 band crossing is thus characterized by a sharp cusp in the inverse mass dependence, as seen in Figs. 5 and 6, and the strain for which the levels are degenerate can be identified by the second change in sign of the heavy-hole effective mass.

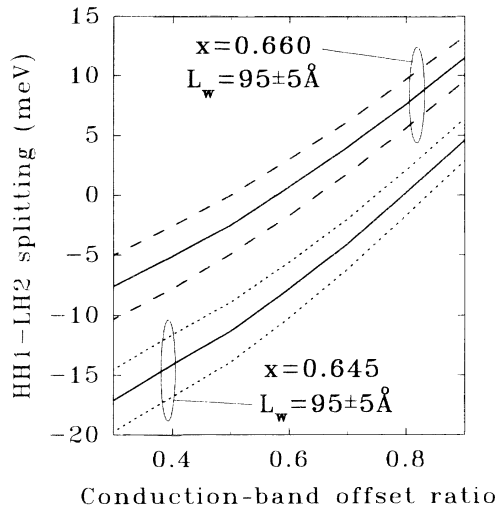

FIG. 8. The splitting of the HH1 and LH2 levels calculated as a function of the conduction-band offset ratio for $In_{1-x}Ga_xAs$/InGaAsP structures with $x = 0.66$ and 0.645.

The observed cusp in the inverse heavy-hole mass therefore enables an estimate to be made of the band offset ratio for the tensile strained structure where the LH2 and HH1 levels are degenerate. Figure 6 indicates that this occurs for an $In_{1-x}Ga_xAs$ well with $0.645 < x < 0.66$ ($1.21\% < \varepsilon_{well} < 1.29\%$). The HH1-LH2 separation calculated using a range of conduction-band offset ratios for $x = 0.645$ and 0.66 is shown in Fig. 8. In order to estimate the consequences of uncertainties in the layer thicknesses, widths of 93 and 97 Å are also used, with the MQW period held constant. For a well width of 95 Å the condition of zero separation of the HH1 and LH2 levels leads to an estimate of 0.68 ± 0.10 for the conduction-band offset ratio ($\Delta E_C / \Delta E_{G,\mathrm{HH}}$, with the band gap taken as that of the heavy holes). Uncertainties of ±2 Å in the well width are seen to lead to $\pm(5-7)\%$ uncertainties in the estimates of $\Delta E_C / \Delta E_{G,\mathrm{HH}}$, but even the lowest limit is much greater than 0.4, which is a characteristic value for comparable lattice-matched combinations. A number of different measurements of band offsets have returned values for $\Delta E_C / \Delta E_{G,\mathrm{HH}}$ close to 0.39 (±0.02) for a wide range of lattice-matched In(Ga,As)P heterojunctions, including $In_{1-x}Ga_xAs$/InP, InGaAsP/InP,[15] $In_{1-x}Ga_xAs$/InGaAsP,[16] and InGaAsP/InGaAsP.[17] Few estimates of $\Delta E_C / \Delta E_{G,\mathrm{HH}}$ for strained material have been reported but our magneto-optical studies of InGaAsP/InGaAsP (Ref. 17) and $In_{1-x}Ga_xAs/In_{1-x}Ga_xAs$ (Ref. 18) strain-compensated structures with $\approx 1\%$ compressive strain in the wells, have given values close to 0.5 in both cases. Along with the estimate of $\Delta E_C / \Delta E_{G,\mathrm{HH}} \approx 0.68$ reported here for the tensile strained $In_{1-x}Ga_xAs$/InGaAsP structure, this indicates that strain of either sense can increase $\Delta E_C / \Delta E_{G,\mathrm{HH}}$ above its value in lattice-matched material.

The values of $\Delta E_C / \Delta E_{G,\mathrm{HH}}$ estimated for the measured samples using the model solid theory with interpolated "average" valence-band positions, as described above, suggest a gradual decrease from 0.35 to 0.20 as the strain in the quantum well changes from 1% compressive to 1.6% tensile. For the samples discussed in the preceding paragraph ($1.21\% < \varepsilon_{well} < 1.29\%$) the calculation estimates $\Delta E_C / \Delta E_{G,\mathrm{HH}}$ to be approximately 0.25. The measured values for the strained InGaAs(P)/InGaAsP structures are seen to be in strong contradiction with those predicted by the model solid theory for both compressive and tensile strain. This intriguing result suggests possible further advantages for the use of strain in optoelectronic devices by the engineering of favorable band offsets. The band offset ratio has important consequences for the design and operation of quantum-well devices, affecting the confined energy levels and the tunneling rates for the carriers. For example, the large valence-band offset in lattice-matched $In_{1-x}Ga_xAs$/In(Ga,As)P-based optical modulators leads to saturation problems due to the trapping of photogenerated holes within the wells. We propose that biaxial strain can be used to increase $\Delta E_C / \Delta E_{G,\mathrm{HH}}$ and counteract this problem. Indeed, electroabsorption modulators fabricated from the compressively strained wells discussed in this paper have shown improved saturation performance when compared to comparative lattice-matched modulators.[19] Our measurements also help to account for the increased hole escape rates observed in both compressive and tensile strained InGaAsP/InGaAsP laser structures,[20] without the need to invoke thermal excitation.

CONCLUSIONS

Magneto-optical measurements on a range of strained InGaAsP-based MQW structures have demonstrated dramatic variations in the effective hole masses and excitonic absorption properties. Electronlike in-plane masses are demonstrated for heavy and light holes in structures with different amounts of tensile strain. It is shown that the electronlike hole masses can lead to possibilities of enhanced excitonic absorption coefficients in strained material. The mass dependencies are related to strain-induced nonparabolicities and level crossings in the valence band, and compared with calculated dispersion curves. In particular, evidence of the LH1-HH2 level crossing is demonstrated for tensile strains close to 1.25%, enabling an estimate of 0.68 ± 0.10 for the conduction-band offset ratio in this structure. This result, along with our earlier measurements of compressive strained InGaAsP quantum wells, indicates that $\Delta E_C / \Delta E_{G,\mathrm{HH}}$ is increased by the introduction of biaxial strain, of either sense, in InGaAsP-based MQW's.

ACKNOWLEDGMENTS

This work was supported by a U.K. government LINK program entitled "MOCVD of III/V Materials for Integration" and jointly funded by the SERC and the DTI.

*Present address: Dept. of Physics and Applied Physics, University of Strathclyde, 107 Rottenrow, Glasgow, G4 ONG, United Kingdom.

†Present address: Ludwig-Maximilians-Universität, D-80539 München, Federal Republic of Germany.

[1]J. E. Schirber, I. J. Fritz, and L. R. Dawson, Appl. Phys. Lett. **46**, 187 (1985).

[2]R. J. Warburton, G. M. Sundaram, R. J. Nicholas, S. K. Haywood, G. J. Rees, N. J. Mason, and P. J. Walker, Surf. Sci. **228**, 270 (1990).

[3]E. O'Reilly, Semicond. Sci. Technol. **4**, 121 (1989).

[4]R. W. Martin, R. J. Nicholas, G. J. Rees, S. K. Haywood, N. J. Mason, and P. J. Walker, Phys. Rev. B **42**, 9237 (1990).

[5]R. J. Warburton, R. W. Martin, R. J. Nicholas, L. K. Howard, and M. Emeny, Semicond. Sci. Technol. **6**, 359 (1991).

[6]P. J. A. Thijs, L. J. Tiemeijer, P. I. Kuindersma, J. J. M. Binsma, and T. van Dongen, IEEE J. Quantum Electron. **QE-27**, 1426 (1991).

[7]E. P. O'Reilly, G. Jones, A. Ghiti, and A. R. Adams, Electron. Lett. **27**, 1417 (1991).

[8]M P. C. M. Krijn, G. W. 't Hooft, M. J. B. Boermans, P. J. A. Thijs, T. van Dongen, J. J. M. Binsma, L. J. Tiemeijer, and C. J. van der Poel, Appl. Phys. Lett. **61**, 1772 (1992).

[9]C. G. van de Walle, Phys. Rev. B **39**, 1871 (1989).

[10]M. P. C. M. Krijn, Semicond. Sci. Technol. **6**, 27 (1991).

[11]P. C. Makado and N. C. McGill, J. Phys. C **19**, 873 (1986).

[12]L. Vina, L. Munoz, N. Mestres, E. S. Koteles, A. Ghiti, E. P. O'Reilly, D. C. Bertolet, and K. M. Lau, Phys. Rev. B **47**, 13 926 (1993).

[13]Y. Jiang, M. C. Teich, and W. I. Wang, J. Appl. Phys. **71**, 769 (1992).

[14]M. Silver, W. Barry, A. Ghiti, and E. P. O'Reilly, Phys. Rev. B **46**, 6781 (1992).

[15]E. T. Yu, J. O. McCaldin, and T. C. McGill, in *Solid State Physics,* edited by H. Ehrenreich and D. Turnball (Academic, San Diego, 1992), Vol. 46, p. 1.

[16]S. L. Wong, R. J. Nicholas, C. G. Cureton, J. M. Jowett, and E. J. Thrush, Semicond. Sci. Technol. **7**, 493 (1992).

[17]R. W. Martin, S. L Wong, R. J. Nicholas, A. D. Smith, M. A. Gibbon, J. P. Stagg, and E. J. Thrush, J. Phys. IV (France) Colloq. **3**, C5-327 (1993).

[18]R. W. Martin, S. L. Wong, R. J. Nicholas, A. D. Smith, M. A. Gibbon, J. P. Stagg, and E. J. Thrush (unpublished).

[19]M. A. Gibbon, J. P. Stagg, and E. J. Thrush (private communication).

[20]B. W. Takasaki, J. S. Preston, J. D. Evans, J. G. Simmons, and N. Puetz, Appl. Phys. Lett. **62**, 2525 (1993).